System Trades using the Asymptotic Bode-Step Method

B. Lurie*, A. Ghavimi*, F. Hadaegh†, E. Mettler+

Jet Propulsion Laboratory,
California Institute of Technology
Pasadena, CA 91109-8099

Abstract. The initial stage of a complex system design involves understanding and evaluation of various plant architecture. The conventional approach is to select the configuration of choice via an exhaustive performance evaluation process. The procedure involves designing primitive control laws for each configuration option until the best choice is achieved. This approach is quite time consuming and does not necessarily lead to an optimal choice. An alternative approach is to consider the asymptotic Bode-step technique to arrive at a desired configuration choice. The method is simple and provides a powerful tool in performing system tradeoffs. The method relies on little information regarding plant parameters and does not require any detailed controller design for each system configuration option. The method can easily lend itself to an optimized control strategy that is applicable during both the initial and the final stages of a concept design. The procedure is demonstrated by applying the proposed method to the motion control design of the retroreflector carriage of a spacecraft instrument.

1. Introduction

The initial stage of a concept design requires understanding of plant properties for multiple system architecture. System dynamics are not well understood, and plant parameters, e.g., frequency and damping of structural modes, sensor type and limitations, actuator type and limitations, sensor and actuator numbers and locations, are not well defined. The selection process for the configuration of choice is usually a tedious task and relies heavily on extensive trade studies provided by both mechanical designers and control engineers.

Underrating the control system performance can lead to a highly complex and overly expensive system design. Therefore, the system configuration of choice can not be finalized before the control systems design is optimized. On the other hand, ignoring issues related to system structural dynamics and the associated plant parameters can also lead to either a costly design, or even an unrealizable one. Therefore, the control system design can not be finalized before the architectural and implementation issues are resolved. That is, neither can hardware designers, nor can control engineers individually dictate a design. In general, appropriate selection of plant parameters is a tedious task and requires extensive interactions between mechanical designers, system engineers, and control engineers to assess the available control performance for multiple system configurations. Such interactions are essential to arrive at a simple and viable system design. This problem is known as control-structure interaction and is depicted in Figure 1.

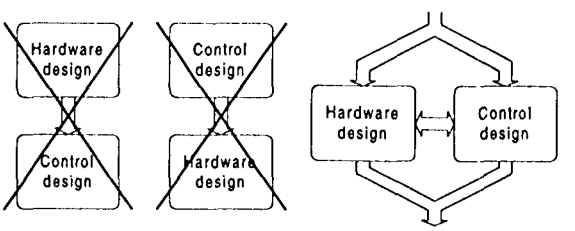

Fig. 1. Control-structure interaction

The control-structure interaction problem may be trivial when a system design is based heavily on a previous design heritage. On the other hand, the control-structure interaction problem can be quite complicated for a new system design. The conventional approach is to find the desired configuration option by means of exhausting iterations as no other practical method yet exists. The strategy is to evaluate the control performance of multiple system architecture by designing preliminary PID-based control laws for each case. The process generates a system trade matrix

---

* Senior Technical Staff
† Senior Research Scientist, Associate Fellow AIAA
\+ Senior Technical Staff, Senior member AIAA

through which the configuration options are narrowed. The remaining choices are evaluated further by applying more detailed control analysis until the final choice is achieved. Despite the simple nature of the process, the approach is quite time-consuming and does not necessarily lead to an optimal design. A different approach is to employ a more sophisticated controller design methodology during the evaluation process; however, the scheme can be quite costly and has little practical feasibility. The main objective of this paper is to propose a simple and powerful tool that is capable of simplifying this tedious design iteration process. The strategy is to evaluate the configuration options via the application of the asymptotic Bode-step method. A system trade matrix is then constructed to facilitate the selection process. Once the final choice is selected, an optimal controller can be designed based on information derived from the associated Bode diagram that was used in the final stage of the selection process.

The proposed design process is especially suited for NASA novel space systems where the conceptual design and simulation must be done by NASA engineers and the detailed design and manufacturing is done by private industry.

2. System trades by PID controllers

Figure 2 illustrates the flow-chart representation of a typical control system design process. The diagram shows that a concept design is studied by examining multiple architectures where each version is also broken up into multiple configuration options. The overall control performance must be evaluated for every individual subversion whose specifications may require the implementation of multiple servo loops. The conventional approach is to evaluate the available control performance of these configuration options by designing preliminary PID-based control laws for each case. Once a system trade matrix is obtained, the configuration options are narrowed to a smaller set, and the remaining choices are evaluated further by more detailed control analysis until a final design is achieved. The corresponding control laws are improved further by standard control-related techniques, e.g., tuning the system to certain operating conditions, inclusion of possible feedforward methods, or implementation of nonlinear feedback compensation. A better controller design is typically postponed for the final choice of the system configuration since higher performance controller design in the early stage of a design process is commonly believed to be impractical and unjustified, especially, for the case that a design option that is not final and may be subject to rejection.

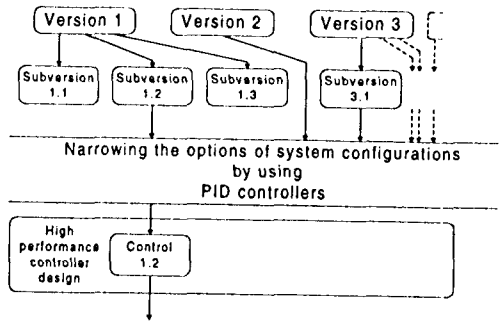

Fig. 2. Conventional system trade of a concept design.

PID-based controller designs are simple; however, they do not provide a systematic procedure for assessing the required control performance, stability, and disturbance rejection. Moreover, the approach requires designing separate controllers for each system configuration option. In addition, the final loop design in each case is not unique, and this makes it difficult to evaluate the resulting trade matrix in a unifying framework. Another important concern is the validity of the results. The difference in disturbance rejection between the PID and a high-performance controller can exceed 10 and even 20 dB [3], especially, when plants have uncontrollable flexible modes. Therefore, the trade-off information obtained from a preliminary PID-based design is often erroneous. For example, the system configuration "A" performs better than "B" when PID controller methods are employed in both cases, where, in fact, System "B" is more preferable when a high-performance controller design is employed. In this respect, a preliminary PID-based design can lead to hardware design complications, substantial cost impact, or even major system configuration change at a later stage of the design process.

3. Asymptotic Bode-step methods

Bode-step method is based on Bode integrals that were developed in connection with the conceptual design of wideband feedback amplifiers.

The first Bode integral formula is described by

$$\int_{-\infty}^{\infty} \ln|F|\, d\omega = 0,$$

where $F = 1 + T$ and T is the negative of the loop transfer function. The feedback at any specific frequency ω, is called *negative* when $|F(\omega)|>1$, and *positive* if $|F(\omega)|<1$. The above integral formula implies that the area of the negative feedback is equal to the area of positive feedback over the range of all frequencies as is illustrated in Figure 3.

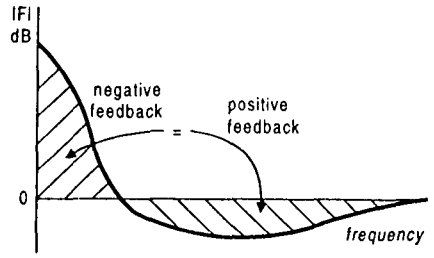

Fig. 3. Feedback as a function of frequency.

One of the primary objectives of a control system design is to maximize the area of negative feedback to achieve maximum disturbance rejection over a specified frequency range, typically known as the *operational bandwidth*. The above formula implies that the negative feedback area is maximized if and only if the positive feedback area is maximized. The positive feedback region generally has most of its concentration near the crossover frequency f_b, i.e., where $|T(2\pi f_b)| = 1$. Therefore, a proper loop shaping in the vicinity of f_b is essential for achieving maximum negative feedback over the desired functional frequency bandwidth.

The value of the feedback is best understood in terms of Nyquist diagram and is given by the distance from the critical point (-1, 0j) to the loop gain transfer function at any given frequency. In light of the above integral formula, it then follows that the area of negative feedback is maximized as long as the distance of the Nyquist diagram of the loop gain transfer function to (-1,0j) is minimized over the frequency range of the positive feedback. This implies that the Nyquist diagram must follow the prescribed stability margin boundaries as close as possible. Note that the stability margins are defined in terms of possible plant parameter variations and minimum requirements on allowable degrees of process instability [2, 4]. The area is typically described by a rectangle on the logarithmic Nyquist plane as shown in Figure 4.

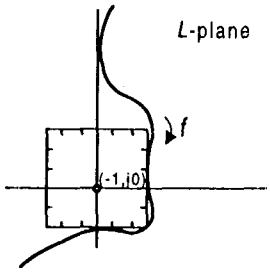

Fig. 4. Stability margin

The second Bode integral formula is known as Bode phase integral [1, 2, 4]. This formula has important design implications and describes tradeoffs between the loop phase lag and the available control performance (disturbance rejection) over the operational bandwidth. Let (A', φ') and (A'', φ'') represent the gain and phase response pair of two minimum phase transfer functions that have similar high frequency characteristics. Figure 5 illustrates the spectrums as a function of frequency. The Bode phase integral is then defined by

$$\Delta A_0 = (A_0'' - A_0') = -\frac{1}{\pi}\int_{-\infty}^{\infty}(\varphi'' - \varphi')\, du,$$

where u is the logarithmic frequency, $(A_0'' - A_0')$ is in Nepers, and $(\varphi'' - \varphi')$ is in radians.

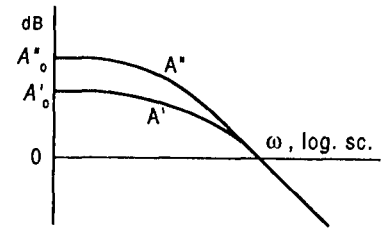

Fig. 5 Spectrum of minimum phase transfer functions

The above formula implies that the value of feedback over the operational frequency bandwidth is directly proportional to the value of the associated phase lag. This means that the larger the phase lag, the greater the feedback is in the working band. In other words, the available disturbance rejection is maximized if the loop phase lag is maximized at all frequencies. On the other hand, the global stability considerations limit the amount of phase lag and consequently, limit the amount of available feedback.

The third Bode integral formula is known as the Bode phase-gain integral [1,2,4] and is described by

$$\phi(\omega_0) = \frac{1}{\pi}\int_{-\infty}^{\infty}\frac{d(\ln|T|)}{du}\ln(\coth\frac{|u|}{2})du,$$

where $\phi(\omega_0)$ is the associated phase of the loop gain T evaluated at the frequency ω_0, and $u = \ln(\omega/\omega_0)$. The above integral implies that the loop phase at any given frequency is a weighted functional of the loop gain slope at all frequencies. At a closer look, it is seen that $\ln(\coth |u|/2)$ scales the gain slope heavily only at frequencies to within a decade on either side of the frequency point, where the phase is being evaluated. By further manipulation of the above formula, it can be shown that for a loop gain with

constant slope of $6n$ dB/octave, the phase can be approximated by 90n degrees. This gives a useful guideline in shaping the open-loop gain for a specified phase stability margin. Specifically at higher frequencies, a steep roll-off is usually desired to attenuate the effects of sensor noise and structural modes. However, the third integral formula indicates that such a loop shape at high frequencies may result in excessive phase lag at the crossover frequency and ultimately leads to instability. This undesired effect can be remedied by designing the loop gain to include a flat piece that extends for 1 or 2 octaves below the 0 dB level by a prescribed gain margin. This flat segment of the response is known as the *Bode Step* and plays a crucial part in satisfying the high-frequency roll-off requirements and the phase stability margin limitations. Figure 6 presents an sketch of the Nyquist diagram in the L-plane for a square stability margins.

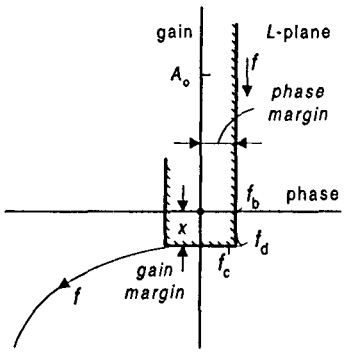

Fig. 6. Bode diagram with Bode step

Figure 7 illustrates the Bode diagram representation of the above Nyquist diagram. This diagram may be viewed as a transcendental function; however, it can be approximated closely with a high-order rational function for the sake of both detailed design evaluation and controller design implementation.

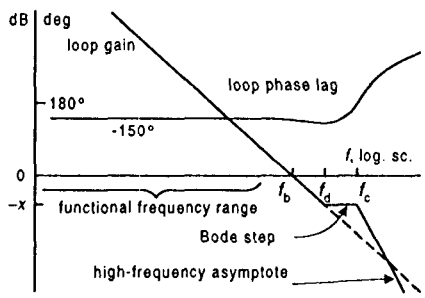

Fig. 7. Asymptotic Bode diagram with Bode step

4. System trades by asymptotic Bode-step methods

This section describes the application of the Bode integrals for evaluating the performance of multiple system configuration option. The method is applicable to mechanical servo systems and requires only approximate knowledge of structural modes together with the system performance requirements. The method is capable of rapidly predicting information on the available feedback bandwidth, the available disturbance rejection, the required sensor and actuator bandwidth and resolutions, and the required sampling frequency if a digital implementation is desired. Moreover, once the system architecture is finalized, a high-performance controller can easily be realized from the resulting Bode-step design approach. This, in turn, shortens the end-to-end life cycle of a concept design and provides a simple, viable, and inexpensive solution. The method is by far more advantageous over the conventional approach since it eliminates the number of design iterations. The initial selection process of a conceptual design can be summarized as follows.

Asymptotic Bode Step Algorithm:

1. Define desired values for phase and gain stability margins, $180y$ degrees and x dB, respectively. Typically, $y = 1/6$ and $x = 10$ dB.
2. Approximate the slope of the open-loop gain in the low-frequency range by $-12(1-y)$ dB per octave.
3. Choose the slope of the loop shape for high-frequency range to account for sensor noise, plant uncertainties, structural modes, and sampling frequency discretization. The typical value is -18 dB per octave.
4. Estimate the frequency f_{st} and damping ξ of the lowest and dominant structural mode for each system configuration option.
5. Draw the high-frequency asymptote for each case such that each line pass through a corresponding point whose associated frequency and gain are f_{st} and $-(x + 20\log_{10}Q)$, where $Q = 1/\xi$.
6. Find the frequency f_c that corresponds to a point with the gain $-x$ on the above asymptote.
7. Draw the Bode step as a flat segment whose end point is f_c, its starting point is f_d, and its width is 1 octave. If the slope of the high-frequency roll-off corresponds to a third-order pole or less, 1 octave is usually sufficient; otherwise, the Bode step width should be about 1.2 octaves.
8. Once f_c is determined in Step 7, draw the low-

frequency asymptotic line such that it passes through the starting point of the Bode Step with a slope that was determined in Step 2. Find the crossover frequency f_b, where the line crosses the zero dB level.

9. Assess the available control performance for each system configuration option.
10. Once choices are narrowed, approximate the associated Bode plots by rational transfer functions. Extract controller transfer function for each particular plant. Perform simulations to provide additional bases for tradeoffs.

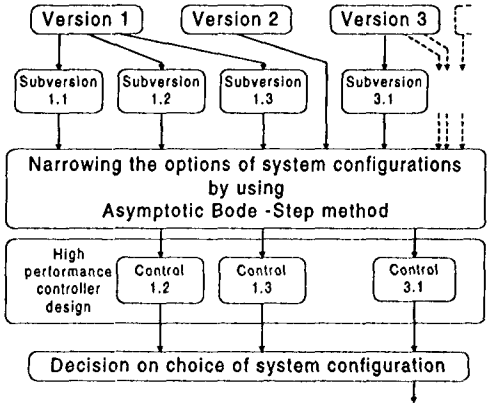

Fig. 8. Proposed evaluation of a concept design.

5. A conceptual design example

The proposed Bode step algorithm has been employed in the design process of the retroreflector carriage of a spacecraft interferometer subsystem, depicted in Figure 9. The corner cube of the carriage is required to translate back and forth to vary the optical paths lengths of an optical interferometer. The motion of the translator is cyclic and is expected to accelerate from rest and settle to a constant rate of nearly 1 cm/sec over 0.3 seconds and maintain the rate for 4 seconds and sometimes for 16 seconds and come to rest over 0.3 seconds. The motion then repeats. The performance of this subsystem is most stringent in rate and is required to follow the constant scan rate with a velocity ripple of no more than ±3 %.

The carriage has several structural modes that are related to the longitudinal mode of the cable (about 100 Hz), bending mode of the rollers (about 116 Hz), and the rocking mode of the rollers (about 96 Hz). The average moment of inertia reflected to the motor axis is about 0.02 kgm^2. The motor drum radius is approximately 4 cm.

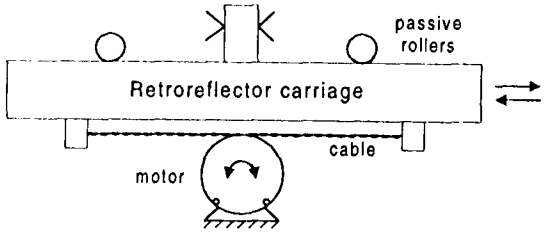

Fig. 9. Retroreflector carriage design

The preliminary control system design must assess performance for a set of mechanical plants with different structural modes and various friction characteristics. The data must be provided to system designers to choose appropriate encoder, motor, electronics, bearings type and preloads, and key elements in the supporting structure.

6. Determination of the available feedback

Figure 10 shows a block diagram representation of the feedback control. The encoder data is sampled at 100 Hz and is used to calculate the input to the motor without substantial delays. Since the sampling frequency is of the same order of the structural resonance, the resulting LTV system has substantial phase uncertainty at the frequency of the structural modes. Therefore, the mode must be gain-stabilized.

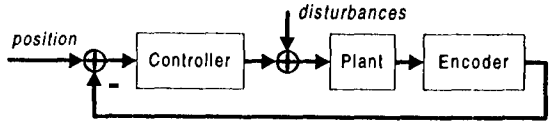

Fig. 10. Block diagram of the feedback loop

As was stated earlier, the feedback bandwidth f_b is generally limited by sensor noise, sampling period, and plant structural modes. The encoder accuracy in this example is quite high. Therefore, the resulting quantization noise is not expected to impact the feedback bandwidth or shaping of the loop gain. The sampling frequency, however, limits the bandwidth. The conventional rule of thumb is to set the feedback bandwidth to be less then 10-15% of the sampling frequency, i.e. less than 10-15 Hz. To determine the effects of the structural modes, the gain and phase stability margins are selected to be the typical values of 10 dB and 30 degrees, respectively.

As a result, the slope of the open-loop gain in the low-frequency range is about -10 dB per octave. The next step is to select the high-frequency roll-off. In this example, it is sufficient to characterize the high-

frequency loop shape by a third order pole, or equivalently, -18 dB per octave roll-off. This, together with the lowest frequency of the structural modes, implies that the feedback bandwidth f_b must satisfy

$$f_b < 0.25 f_{st} Q^{-1/3} = 0.25(96)(100)^{-1/3} \approx 5.2 \text{ Hz}.$$

It then follows that the structural modes have the most impact on the feedback bandwidth. Therefore, the crossover frequency f_b is set to be 5.2 Hz. Figure 11 illustrates the resulting loop gain design.

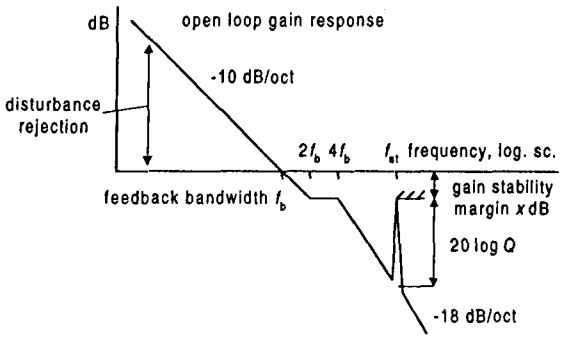

Fig. 11. Asymptotic Bode diagram

As is seen, the above procedure easily constructs a loop design based on minimal information on structural modes and a target stability margin. The information from the above loop design can be studied further to estimate the time response characteristics like rise time and settling time without the actual design of the control laws. The loop design can easily be redesigned for different values of frequency and damping of structural modes. Figure 12 demonstrates the trade-off results for different values of the frequency f_{st} and the quality factor Q. It is seen that as f_{st} decreases or Q increases, the available feedback bandwidth, and consequently, the available disturbance rejection decreases. As a result, the rise time increases which in turn degrades that available control performance.

As an example, suppose that the motor used in the servo loop has 45 slots. Then, the resulting motor reluctance cogging torque is a disturbance torque whose frequency is about 2 Hz for the specific scan rate of the servo system. If the control bandwidth is 4 Hz, the cogging disturbance torque is *amplified* by positive feedback in the crossover area by about 2 times. However, for a control bandwidth of 10 Hz, this disturbance torque is *attenuated* by about 2 times. The difference in these two cases is about 12 dB. Such a difference is significant and serves as a motivating factor in the hardware selection process.

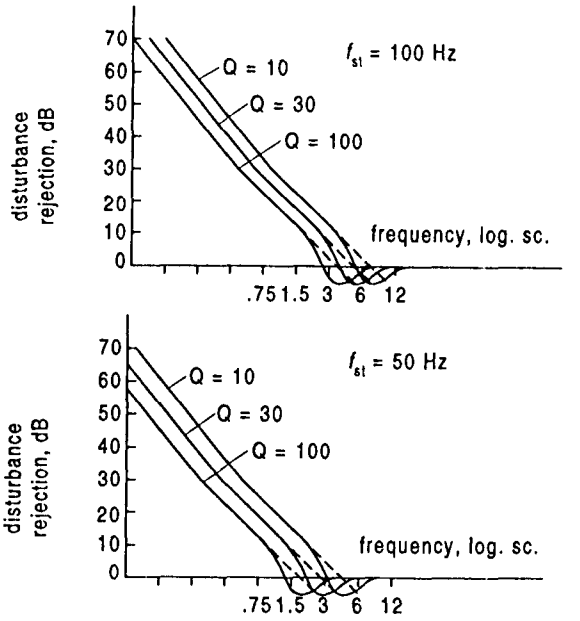

Fig. 12. Sensitivity results for different values of frequency and damping of the structural modes.

7. Controller design

The application of the asymptotic Bode method is capable of reducing the number of available configuration options during the initial phase of a concept design. To finalize the particular choice of hardware, a more detailed analysis must be conducted that includes the effects of friction, uncertainties, sensor noise, unmodeled dynamics, phase delay, and discretization.

The asymptotic Bode diagram developed in the previous section can be approximated with rational transfer functions. Figure 13 shows the plot of the normalized transfer function

$$\frac{1}{s^2} \frac{11s^3 + 55s^2 + 110s + 36}{s^4 + 7.7s^3 + 34s^2 + 97s + 83},$$

with the crossover frequency of 1 rad/sec, a Bode step of approximately 1 octave long, a low-frequency asymptotic slope of −10 dB per octave, a high-frequency asymptotic slope of −18 dB per octave, a gain margin of 10 dB, and a phase margin of 30 degrees [4]. Figure 13 shows the associated Nyquist diagram in the L-plane. It is then an easy task to extract a controller transfer function from the above loop design.

Suppose the normalized plant is represented by $1/s^2$. In addition, a nonminimum phase lag is also included in the plant model to account for the effect of sampling period. In this setting, the normalized plant transfer function is given by

$$P(s) = \frac{1}{s^2}\frac{10-s}{10+s}$$

and the corresponding normalized controller is

$$C(s) = \frac{11s^3 + 55s^2 + 110s + 36}{s^4 + 7.7s^3 + 34s^2 + 97s + 83}.$$

Therefore, the normalized loop transfer function is

$$T(s) = C(s)\frac{1}{s^2}\frac{-s+10}{10+s}.$$

The controller *C(s)* can be decomposed further into the sum of two parallel cascades of low-pass and high-pass transfer functions as shown in Figure 14.

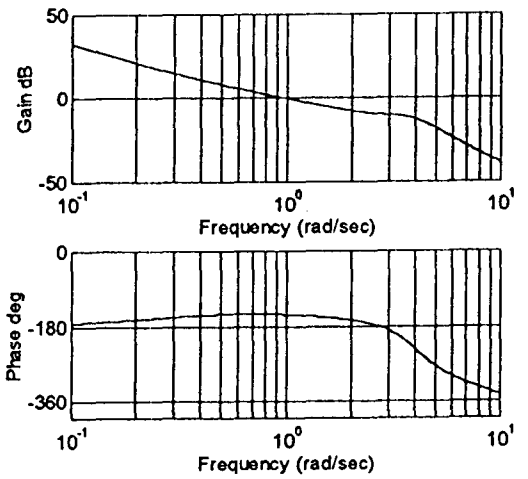

Fig. 12. Normalized open-loop response

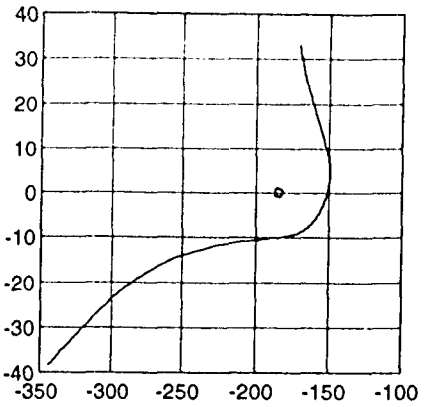

Fig. 13. Normalized *L*-plane Nyquist diagram

The normalized prefilter function is

$$R(s) = \frac{s^2 + \omega_b s + 0.81\omega_b^2}{s^2 + 2\omega_b s + 0.81\omega_b^2}\frac{s^2 + 0.5\omega_b s + \omega_b^2}{s^2 + 0.6\omega_b s + \omega_b^2}$$

The functions of the compensator and prefilter were de-normalized for the crossover frequency to be 6 Hz, and the compensator was cascaded with a link

$$\frac{250s + 2050}{s+1}$$

that together with the linearized plant produces de-normalized nominal plant.

8. System model and simulation

The SIMULINK system model is shown in Fig. 14. The friction characteristic is static piece-linear with certain stiction and Coulomb level. The friction model includes saturation links and a summer. The slope of the friction torque can be adjusted with appropriate gain coefficients in the friction model. The coefficients have been chosen for the worst case: the stiction peak duration equals a half period of the oscillation corresponding to the closed loop controller.

Using plots Fig. 11, the feedback bandwidth (the crossover frequency) is chosen to be 6 Hz. The loop response is shaped with a Bode step, with 30° phase guard-point stability margin and 10 dB gain guard-point stability margin, and with −18 dB/oct high-frequency asymptotic slope.

In the simulations we use an motor model with torque constant 0.32 Nm/A and 1.7 Ω winding, with 4% torque variations as a function of the angle, with 45 slots, and with 0.01 Nm peak-to-peak ripples in the torque (of cogging). The plant equivalent moment of inertia relative to the shaft of the motor is 0.02 kgm^2.

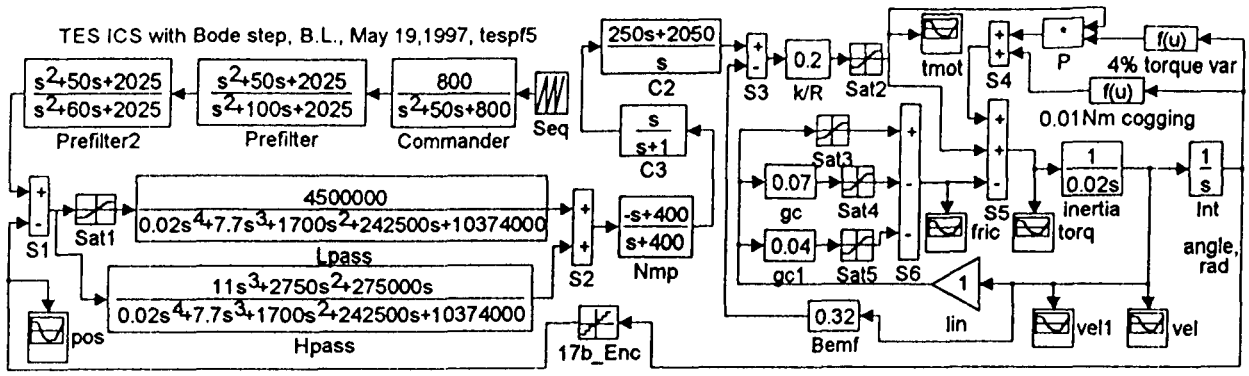

Fig. 14. System model; the structural resonances not shown

The motor is driven by a voltage source, so that the relatively low motor winding resistance serves as the output impedance of the driver. As can be shown, in this case the motor cogging and torque variations have lesser effect on the controlled variables.

The compensator transfer function is splitted into low-frequency and high-frequency parallel paths. In front of the low-frequency path a saturation is placed with threshold 0.1 to improve the transient response to large amplitude commands and to provide global stability. The prefilter in the command path includes two notches tuned at the frequency close to the crossover. The link $(-s + 400)/(s + 400)$ represents the phase delay associated with the sampling.

The simulation results are shown in Figs. 15-18. As seen in Fig. 15, the turn-around angle of 0.064 rad is covered in 0.3 sec. As seen in Fig. 16, angular velocity becomes constant as desired with better than 3% accuracy in approximately 0.15 sec. On the velocity time-history, the ripples at times up to 0.3 sec are from the controller closed loop response. The lower-frequency ripples at larger times are from the cogging (the cogging will be smaller with an appropriate motor).

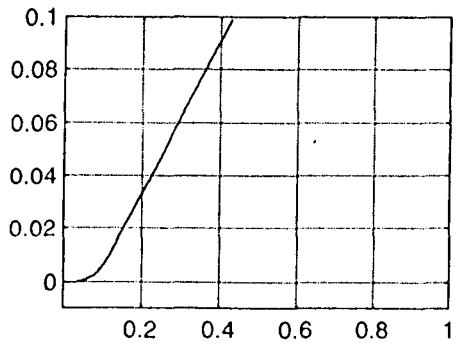

Fig. 15. Angle, rad

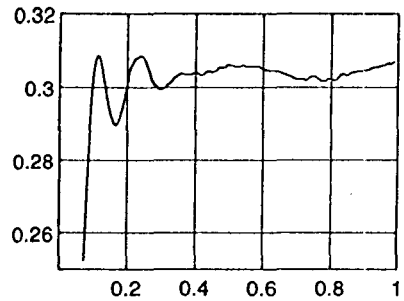

Fig. 16. Angular velocity, rad/sec

The motor torque time-history is shown in Fig. 17.

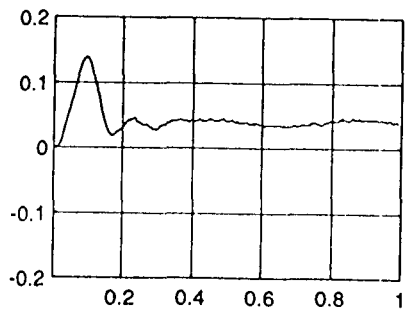

Fig. 17. Motor torque, Nm

The stiction and Coulomb torque seen in Fig. 18.

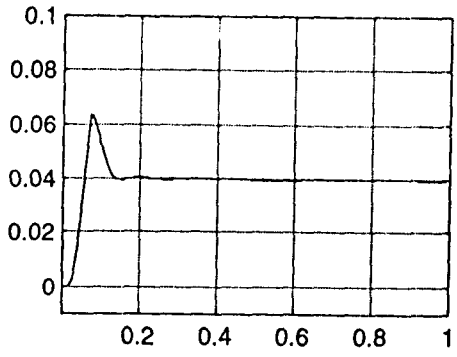

Fig. 18. Friction torque, Nm

Without friction, the velocity time history is shown in Fig. 19. The velocity settles to the required accuracy in 0.2 sec.

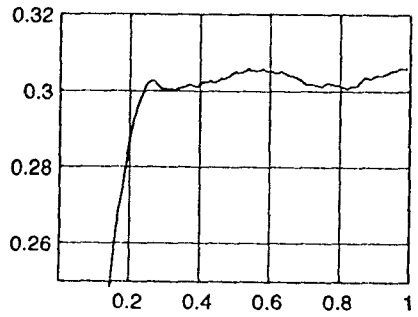

Fig. 19. Velocity plot when friction is absent

9. Flexible mode

From Fig. 3 it is seen that the chosen crossover frequency of 6 Hz corresponds to the flexible mode 100 Hz with Q of 15. However, the modes in the plant are collocated, and due to the ratio of participating masses the poles will be rather close to zeros, say, within 20% in frequency. Then, the control system should be stable even with lower frequency of the flexible mode and with higher Q.

A collocated flexible mode with the frequency of the poles 60 Hz, of the zeros 50.3 Hz, and 0.01 damping was introduced in the plant as a cascaded link after the inertia link with transfer function

$$\frac{s^2 + 6.3s + 100000}{s^2 + 7.5s + 142000}.$$

The flexible mode (the poles) are substantially damped by the low output impedance of the driver transformed into low output mobility of the motor. However, when the driver is saturated, the damping effect decreases, and a system without substantial attenuation in the loop gain can be only conditionally stable and have a limit cycle. For this reason, substantial loop gain attenuation at the pole frequency provided by the Bode Step response is necessary.

The results of the obtained system simulation are very similar to those for the system without structural modes; the system remains stable.

Conclusions

The proposed method eliminates the need for designing control laws or designing a high-fidelity model in order to estimate the utmost available performance of a system during the initial design process. In addition, the method provides a simple tool for the extraction of a final controller design from a resulting optimal loop response in the final stages of a control system design.

Acknowledgment.

The research was carried out by the Jet Propulsion Laboratory, California Institute of Technology, under a contract with the National Aeronautic and Space Administration. The authors thank Drs. R. Laskin and E. Wong for discussions.

References

1. H. W. Bode, *Network Analysis and Feedback Amplifier Design*. Van Nostrand, N.-Y., 1947.
2. B. J. Lurie, *Feedback Maximization*. Artech House, Dedham, Ma: 1986.
3. B. Lurie, R. Laskin, E. Wong, JPL Engineering Memorandum 343-1165, 1990.
4. B. Lurie and P. Enright, *Advanced Classical Control*, manuscript, 1998.